Analysing the Pressure Effect on the Contact Resistance of Electrical Connections

Jordi-Roger Riba[1] and Pau Bas-Calopa[2]

[1] Universitat Politècnica de Catalunya, Terrassa, Spain

E-mail: jordi.riba-ruiz@upc.edu

Received xxxxxx
Accepted for publication xxxxxx
Published xxxxxx

Abstract

We propose an experiment intended for undergraduate laboratories, with the aim to introduce different novelties as a subject for a practical session or students project. We deal with the different components of the resistance in an electrical connection, with special focus on the contact resistance and its dependence with the applied mechanical load or pressure at the interface, since for a fixed geometry and connection materials, the contact pressure has a leading role on the final value of the resistance. The topics analysed are suitable for students with intermediate knowledge of physics. The dependence of the electrical resistance of two metallic rough surfaces with the applied pressure is studied and measured in the laboratory, and the weight of their different components is determined from calculations, simulations and measurements. The pressure dependence of aluminium and copper contacts have been analysed, since they are the most commonly used materials in electrical connections.

Keywords: electrical resistance, contact resistance, electrical connections

1. Introduction

Electrical connections or joints play a key role in electrical circuits and systems. Loose connections can generate excessive thermal losses and hot spots due to an unacceptable increase of the contact resistance, so they can lead to safety issues and ultimately to arcing and fire hazards. The contact resistance of electrical connections has a deep impact on their thermal behaviour, stable operation, efficiency, long term performance and useful life [1,2]. The analysis of the contact resistance requires applying basic mechanical and electrical concepts. The contact resistance of an electrical connection relies on different factors such as the apparent contact area [3], the distribution and morphology of the conducting spots formed at the contact interface [4] and the applied contact pressure [5]. Factors such as the applied pressure and the condition of the contacting surfaces, including the roughness of the matting surfaces, greatly determine the real area of contact and the density and distribution of the conducting spots. The real area of contact between two rough surfaces, i.e., where the electrical interaction between the two contacting surfaces occurs, is much smaller than the nominal or apparent contact area, usually below 1% of the nominal contact area [6].

The most common ways to make electrical connections between conductors is by means of fusion (welded, soldered or brazed connections) or pressure (clamped or compressed connections). This paper applies to clamped or compressed connections, which are the most commonly applied methods.

To make a good connection, a high enough contact pressure must be applied in order to generate a sufficient contact area as to allow a continuous electrical current transfer across the contacting interfaces. By ensuring a suitable contact pressure, the temperature in the contact are reduced [7] because of the decrease of the contact resistance due to the pressure effect on the asperities found in the contacting interfaces, which reduce the real contact area [8].

The applied pressure deforms the asperities and increases the real contact area [9].

The contact resistance of rough surfaces has often been described by applying methods based on multiscale, fractal or statistical approaches [10]. Multiscale models consider the elastic-plastic behaviour of the contact area. Fractal approaches take into account the multiscale behaviour of contact surfaces. Statistical models focus on the stochastic nature of contact surfaces [11], although they do not consider their multiscale nature [10]. The multi-physics behaviour of rough contacting surfaces can also be studied by means of the finite element method (FEM) [10,12].

Due its complex origin, there are no analytical formulas to describe the contact resistance of solid interfaces [13]. This paper develops an approach to determine the effect of pressure on the different components of the electrical resistance in an electrical connection combining analytical equations, FEM simulations (optional) and experimental measurements. Although a particular contact geometry is analysed, this method can be generalized to other geometries. The proposed approach is suitable to develop a transversal project involving mechanics and electricity for undergraduate laboratories. Despite the leading role of the contact resistance in electrical connections, this topic is rarely studied in regular courses, thus a practical session or students project analysing this topic could help overcoming this issue.

This paper is organized as follows. Section 2 details the components of the electrical resistance in a joint and the way to find them. Section 3 explains the effect of pressure on the contact resistance. Section 4 quantifies mechanical elongation and effects of thermal on the resistance of the joint. Section 5 summarizes the approach applied in this paper to determine the contact resistance, Section 6 details the experimental setup, Section 7 presents the results attained and, finally, Section 8 concludes this work.

2. Components of the electrical resistance in a joint

This section describes the components of the electrical resistance of the connection.

Fig. 1 shows the geometry of the aluminium and copper samples analysed in this work, as well as the distribution of the current lines along the samples.

The resistance in an electrical connection has two main terms, the bulk resistance and the contact resistance,

$$R_{total} = R_{bulk} + R_{contact} \quad (1)$$

The bulk resistance mainly depends on the geometry and material of the contact. It has two terms, the geometrical resistance $R_{geometric}$ and the resistance due to the departure of the current lines from a straight line $R_{current\_lines}$ (see Fig. 1b),

$$R_{bulk} = R_{geometric} + R_{current\_lines} \quad (2)$$

It is noted that the bulk resistance term, which includes the geometric resistance and the effect of the redistribution of the current lines, can be obtained from FEM simulations, thus it is denoted as $R_{bulk,FEM}$.

According to Fig. 1a, the geometric resistance between points 3 and 4 can be calculated as,

$$R_{geom} = \frac{\rho}{L_y L_z}(2L_{x1} + 0.5L_{x2}) \quad (3)$$

L_x, L_y and L_z being respectively, the dimensions of the test sample in the three axes and ρ the electrical resistivity of the material in [Ωm].

The $R_{current\_lines}$ term cannot be calculated analytically, so it is calculated from $R_{bulk,FEM}$ as,

$$R_{current\_lines} = R_{bulk,FEM} - R_{geometric} \quad (4)$$

However, as it will be proved in Section 7, the contribution of the $R_{current\_line}$ term is very low.

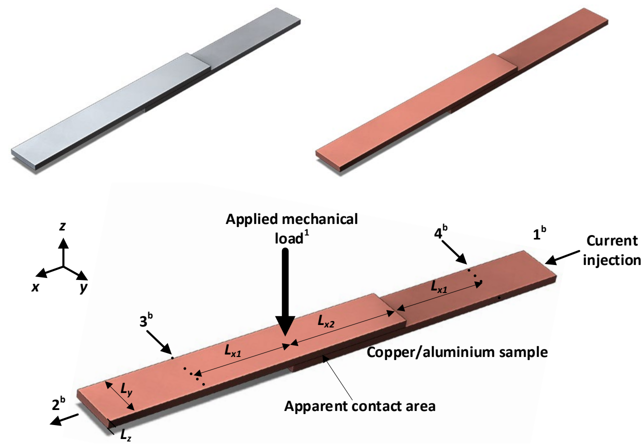

[a] Load applied using a vertical press testing machine
[b] Electrical resistance measured with the four wires or Kelvin method
[b] 1-2: current injection terminals; 3-4: voltage measurement terminals.

a)

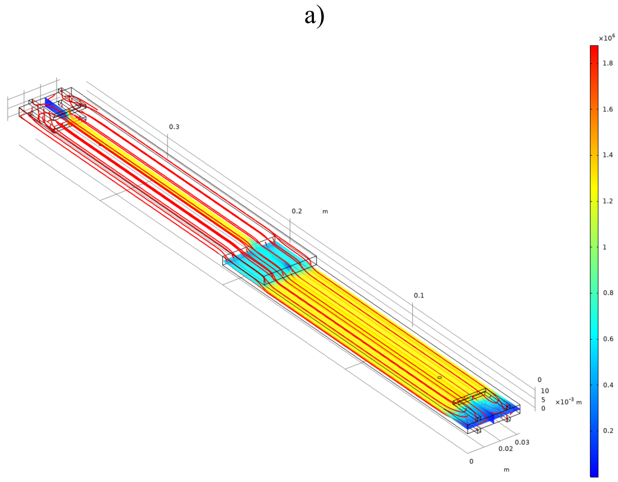

b)

Fig. 1. a) Test sample of aluminium or copper. b) Current density lines in [A/m^2] showing the deviation from the redistribution of the line currents at the interface, thus increasing the effective resistance.

The contact resistance also has two components, the constriction resistance $R_{constriction}$ due to the constriction of the line currents in the spots in the interface, and the film resistance R_{film} due to the oxides and other components formed or found at the interface,

$$R_{contact} = R_{constriction} + R_{film} \tag{5}$$

Both the he constriction effect of the current lines and the oxides formed at the interface tend to reduce the real contact area, so the contact resistance increases. The contact resistance cannot be calculated analytically, so it must be determined from measurements.

3. Effect of pressure on the connection resistance

The conducting spots existing in the contact interface are the only conducting paths to transfer the electric current through the two matting rough surfaces [14]. These spots force the line currents to concentrate or constrict in their surroundings. This uneven distribution of the current lines due to the constriction phenomenon forces the effective resistance to increase, thus raising the constriction resistance term. In the case of aluminium contacts this effect is more pronounced due to the natural growth of alumina (Al_2O_3, aluminium oxide) when aluminium is in contact with atmospheric air, thus contributing to the film resistance term. Alumina is a very good insulating material, and jointly with other possible contaminant elements greatly determines the film resistance component. Thus, the contact resistance includes both components, the constriction and film resistance terms [6].

The constriction and film resistance terms play a leading role in the total resistance because of the dissimilarity between the real and the nominal contact areas. The mechanical load applied to the interface has a deep impact on both terms of the contact resistance and thus, on the total resistance of the contact because of the elastic and plastic deformation produced by the effect of the pressure applied at the interface [8]. The effect of an increasing pressure or compression on the contacting surfaces is to increase the real contact area [10] and the number of spots and their area, thus reducing the contact resistance. When an increasing load is applied to a joint, the contact resistance tends to decrease to a point, beyond which any additional load increase does not produce an appreciable reduction of the contact resistance.

4. Elongation and thermal effects on the resistance of the joint

This section describes the effect of the mechanical compression and the thermal expansion during the test on the resistance of the analysed samples.

4.1 *Elongation due to the mechanical compression*

The mechanical load applied to the contacting interfaces produces a strain, or relative deformation in the direction of the applied load (z axis, see Fig. 1a) is given by,

$$\Delta L_z = -L_0 \frac{F_z}{Y} \tag{6}$$

where F_z is the applied load in the z axis expressed in MPa, Y is the Young or elasticity modulus in GPa, whose values are 70 GPa and 115 GPa for aluminium and copper, respectively. It is noted that (6) is negative because due to the compression effect in the z direction.

In the x and y directions, which are perpendicular to the direction of the applied load, there is also a deformation, which is described by the Poisson ratio as,

$$\begin{cases} \Delta L_x = L_{0x} \dfrac{F_z}{Y} P \\ \Delta L_y = L_{0y} \dfrac{F_z}{Y} P \end{cases} \tag{7}$$

where the Poisson ratio is approximately P = 0.33 for both aluminium and copper materials [15].

The applied load has a maximum value F_z = 30 MPa (the maximum applied load in compression connections is usually below 30 MPa) and the Young modulus is between 70 and 115 GPa. Assuming a square contact area with initial dimensions L_{0x} and L_{0y} and thickness L_{0z}, the expected resistance change under the worst case scenario, due to the elongation effect is calculated as,

$$R_{geom} = \rho \frac{L_x}{L_x L_y} = \rho \frac{L_{0x} + \Delta L_x}{(L_{0y} + \Delta L_y)(L_{0z} - \Delta L_z)} = \begin{cases} 1.00043 R_{geom,0} & \text{for Al} \\ 1.00026 R_{geom,0} & \text{for Cu} \end{cases} \tag{8}$$

$R_{geom,0}$ being the value of the geometric resistance measured at 20ºC with no external pressure applied.

From (8) it is clear that the deformation effect of the mechanical load on the geometric resistance and thus, on the bulk resistance can be neglected, since its contribution is about 0.043% for Al, and 0.026% for Cu.

4.2 *Elongation due to thermal expansion*

The effect of temperature can be described by the equation for linear thermal expansion, which is given by,

$$L = L_0 (1 + \alpha_{thermal} \Delta T) \tag{9}$$

L_0 being the length of the sample in [m] measured at 20ºC, T the temperature of the sample in [ºC], $\Delta T = T - 20$, and $\alpha_{thermal\_expansion}$ the thermal expansion coefficient of the connection material, whose values are $23.1 \cdot 10^{-6}$ K^{-1} and $17 \cdot 10^{-6}$ K^{-1} for aluminium and copper, respectively. Therefore the effect of the thermal expansion in solids is very low [16]. Assuming a temperature increase of 1 ºC in the sample during the test, the thermal expansion effect is almost negligible, since from (3) and (9) the geometric resistance of a square contact area with initial dimensions L_{0x} and L_{0y} and thickness L_{0z} results in,

$$R_{geom} = \rho \frac{L_x}{S_{yz}} = \rho \frac{L_{0x}}{L_{0y} L_{0z}} (1 + \alpha_{thermal\_expansion} \cdot \Delta T) = \begin{cases} 1.000023 R_{geom,0} & \text{for Al} \\ 1.000017 R_{geom,0} & \text{for Cu} \end{cases} \tag{10}$$

According to (10), the effect of temperature on the resistance during the test is also negligible, since its contribution is about 0.0023% for Al, and about 0.0017% for Cu.

From (8) and (10) it is deduced than no further corrections must be applied to the bulk resistance term R_{bulk} due to pressure or thermal effects.

4.3 *Temperature effect on the resistivity*

The electrical resistance of aluminium and copper conductors tends to increase linearly with an increasing temperature as follows [17],

$$R_{geom} = R_{geom,0}(1+\alpha_{resist}\cdot\Delta T) \qquad (11)$$

where α_{resist} is the temperature coefficient of the resistance, 0.0038 K^{-1} and 0.0039 K^{-1} for Al an Cu, respectively.

In order to have comparable results, the resistance is usually converted to 20ºC by applying (11).

5. Procedure To Determine The Pressure Dependence Of The Contact Resistance

This section describes the procedure applied to determine the pressure dependence of the contact resistance, which is summarized in Fig. 2.

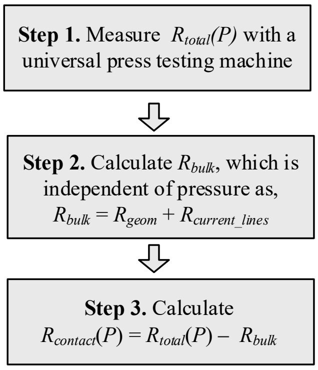

Fig. 2. Flowchart of the six-step procedure proposed in this paper.

As detailed in Fig. 2, the procedure applied in this work to determine the pressure dependence of the contact resistance has three steps. First, the dependence of the total resistance with the pressure $R_{total}(P)$ is measured with the help of a universal press testing machine, while simultaneously the resistance of the test sample is measured by applying the four-wire method explained in Section 6. Next, R_{geom} is calculated from (3), whereas $R_{current\_lines}$ and R_{bulk} are determined from FEM simulations. Alternatively, since the impact of $R_{current\_lines}$ is very low, R_{bulk} can be approximated by R_{geom}. Finally, once $R_{total}(P)$ and R_{bulk} are known, the pressure dependence of the contact resistance is obtained by applying $R_{contact}(P) = R_{total}(P) - R_{bulk}$.

6. Samples analysed and experimental setup

This section describes the samples analysed and the experimental setup.

6.1 *Samples description*

In this work two samples are analysed, i.e., samples made of aluminium alloy and copper. Fig. 1a describes the geometry of the two analysed samples as well as the direction of the applied force and the current injection and voltage measurement terminals.

Table 1 shows the dimensions of the aluminium and copper samples dealt with.

Table 1. Dimensions of the analysed samples

Total length ($L_{x,tot}$)	200 [mm]
Width (L_y)	30 [mm]
Thickness (L_z)	4.9 [mm]
Contact length (L_{x2})	20 [mm]
Distance between voltage probes ($2L_{x1} + L_{x2}$)	280 [mm]

6.2 *Experimental setup*

The test samples were compressed by using a universal press testing machine (maximum vertical compression of 50 kN, model BZ1-MM14780.ZW02 from Zwick Roell, Ulm, Germany). The electrical resistance of the test samples was measured during the mechanical compression tests by applying the four-wire or Kelvin method because of its accuracy, since the readings made by this method are independent of the probes resistance [18]. A digital micro-ohmmeter (current range 10, 20, 50, 100 and 200 A_{DC}, ± 0.01μΩ ± 0.1% reading, model Micro-Centurion II from Raytech, Bremgarten, Switzerland) was used to measure the resistance of the samples, which is in the order of some few tens of μΩ.

Fig. 3 schematizes the experimental setup.

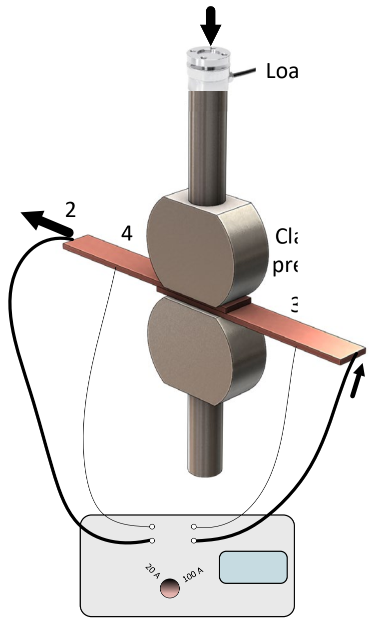

Fig. 3. Experimental setup to compress the samples and simultaneously measure their resistance. The resistance is measured by applying the four-wire method, requiring two terminals for current injection and two terminals for measuring the voltage.

The Joule's law entails a heat production proportional to the product of the square of the electric current by the resistance [19], so the measurement of the resistance must be done by applying a current whose value is low enough to produce a negligible temperature rise of the analyzed sample, but high enough to do not compromise the accuracy in the measurements.

7. RESULTS

This section shows the experimental results obtained in this work with aluminium and copper samples, the most applied materials in electrical connections.

First the bulk resistance terms, i.e., R_{geom} and $R_{current\_lines}$ are found. R_{geom} is calculated by applying (3) and the term due to the redistribution of the current lines is determined as $R_{current\_lines} = R_{bulk,FEM} - R_{geom}$. The results attained are shown in Fig. 4.

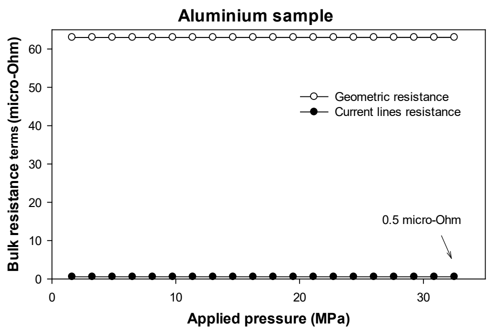

a)

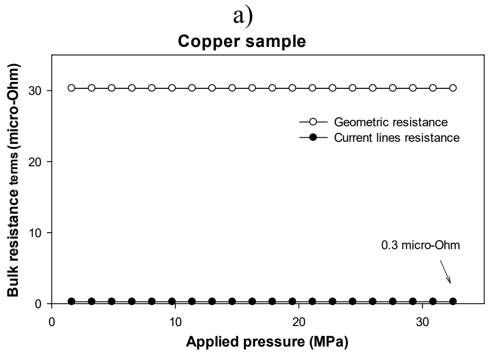

b)

Fig. 4. Bulk resistance terms. a) Aluminium samples. b) Copper samples.

Fig. 4 shows that under the conditions of this work, which are characteristic of real connections, the bulk resistance and its two terms are almost independent of the applied pressure. It is also proved that the $R_{current\_lines}$ term is almost negligible, so that the bulk resistance R_{bulk} term is well described by the R_{geom} term. Since $R_{current\_lines}$ has very little influence on the total resistance, R_{bulk} can be approximated by $R_{bulk} \approx R_{geom}$, so under this approximation, FEM simulations are no longer required. Fig. 4 also shows the higher value of R_{geom} for the copper sample compared to aluminium specimen, due to the lower resistivity of copper compared to aluminium.

Next, the contact resistance term $R_{contact}$ is obtained by subtracting the bulk resistance term R_{bulk} from the measured resistance, so that $R_{contact} = R_{measured} - R_{bulk,FEM}$. The results obtained are shown in Fig. 5.

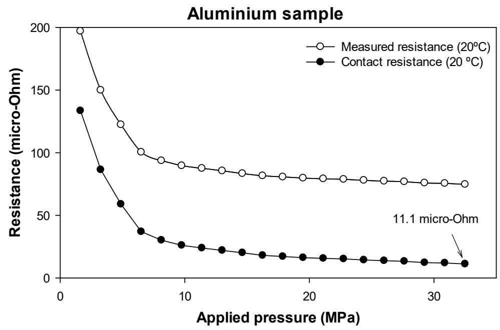

a)

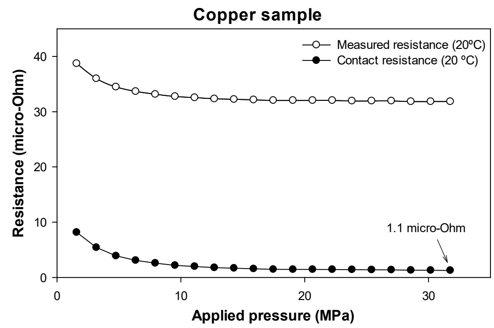

b)

Fig. 5. Pressure dependence of the measured resistance and the obtained contact resistance. a) Aluminium samples. b) Copper samples.

Results presented in Fig. 5 show that the copper sample shows much lower contact resistance than the aluminium sample. This effect is mainly attributed to the most important contribution of the film resistance in aluminium connections because of the formation of a layer of alumina, which is a very insulating material, thus hindering to perform good connections [20]. It is worth noting that it is possible to extend this practical to discern the R_{film} and $R_{constriction}$ terms by applying an acid chemical cleaning treatment to the interface before the experiments. The chemical cleaning allows wiping out the oxide compounds formed at the interface and thus, the R_{film} term is almost removed, thus allowing to separate the R_{film} and $R_{constriction}$ terms.

Results presented in Fig. 5, also corroborate that when applying an increasing pressure, the contact decreases to a point, beyond which any additional pressure increase does not produce an appreciable reduction of the contact resistance. This is because two conductor surfaces in contact never can be perfectly matched [21] because current flows from one surface to the other through a few nanoscopic contact points, restricting current flow and determining the constriction resistance, which greatly contributes to the contact resistance. The effective contact area increases with the applied contact pressure, thus reducing the current flow restriction, and hence the contact resistance. This effect is limited by the properties of the surface material, such as roughness or hardness. As observed in Fig. 5, in the case of copper there is no significant reduction in contact resistance beyond 10 MPa, whereas the contact resistance of aluminium samples is still reduced due to its lower hardness.

Conclusion

The electrical resistance greatly determines the thermal performance and expected service life of electrical connections, so it is of utmost importance to know the relative weight of its components. Despite to its importance in practical applications, this topic is rarely studied in regular courses. This paper has described an experimental approach to determine the effect of pressure on the electrical resistance of an electrical connection. It has been proved that by combining experiment measurements, analytical equations and FEM simulations (simulations are not compulsory), it is possible to determine the different components of the resistance, and to compare the performance of different materials. Results attained with aluminium and copper samples, the most commonly used materials in electrical connections, clearly show that copper offers better connections due to the lower values of the contact and geometric resistance terms compared to aluminium.

The authors of this work consider that the topics analysed in this work are suitable to develop a practical session or students project with transversal contents for undergraduate laboratories, since it involves basic knowledge of mechanics and electricity with low requirements of mathematical concepts. It could be focused to analyse in deep the dependence of the different components of the electrical resistance between metallic contacts with the applied pressure, including the bulk resistance (which also includes the components due to the geometrical resistance and the one due to the departure of the current lines from a straight line) and the contact resistance terms.

Acknowledgements

This work was partially supported by Ministerio de Ciencia e Innovación de España, grant number PID2020-114240RB-I00 and by the Generalitat de Catalunya, grant number 2017 SGR 967.

References

[1] Capelli F, Riba J-R, Rodriguez A and Lalaouna S 2016 Research towards Energy-Efficient Substation Connectors *3rd International Congress on Energy Efficiency and Energy Related Materials* (Oludeniz, Turkey, Turkey) pp 295–301

[2] Kadechkar A, Riba J-R J R, Moreno-Eguilaz M and Sanllehi J 2019 Real-time wireless, contactless, and coreless monitoring of the current distribution in substation conductors for fault diagnosis *IEEE Sens. J.* **19** 1693–700

[3] G. González-Díaz, D. Pastor, E. García-Hemme, D. Montero, R. García-Hernansanz, J. Olea, A. del Prado, E. San Andrés I M 2017 A robust method to determine the contact resistance using the van der Pauw set up *Measurement* **Online** 1–18

[4] Braunovic M 2002 Effect of connection design on the contact resistance of high power overlapping bolted joints *IEEE Trans. Components Packag. Technol.* **25** 642–50

[5] Riba J-R, Mancini A-G, Abomailek C and Capelli F 2018 3D-FEM-Based Model to Predict the Electrical Constriction Resistance of Compressed Contacts *Measurement,* **114** 44–50

[6] Braunovic M, Myshkin N K and Konchits V V. 2006 *Electrical Contacts: Fundamentals, Applications and Technology* (Boca Raton, FL: CRC Press, Taylor & Francis Group)

[7] Bao J, Wu G and Gao B 2016 Research on electric contact calculation and its heat of 500kV transmission line clamps *2016 IEEE International Conference on High Voltage Engineering and Application (ICHVE)* (IEEE) pp 1–4

[8] Robinson A J, Lyons A M and Kempers R 2016 Modelling the effective thermal conductivity of compressing structures including contact resistance *Simul. Model. Pract. Theory* **67** 74–88

[9] Kucharski S and Starzynski G 2014 Study of contact of rough surfaces: Modeling and experiment *Wear* **311** 167–79

[10] Wilson W E, Angadi S V. and Jackson R L 2010 Surface separation and contact resistance considering sinusoidal elastic–plastic multi-scale rough surface contact *Wear* **268** 190–201

[11] Greenwood J A and Williamson J B P 1966 Contact of Nominally Flat Surfaces *Proc. R. Soc. A Math. Phys. Eng. Sci.* **295** 300–19

[12] Pennec F, Peyrou D, Leray D, Pons P, Plana R and Courtade F 2012 Impact of the Surface Roughness Description on the Electrical Contact Resistance of Ohmic Switches Under Low Actuation Forces *IEEE Trans. Components, Packag. Manuf. Technol.* **2** 85–94

[13] Liao, Xiaogang; Li, Renxi; Luo, Weifang; Zhang H 2016 Method for measuring thermal contact resistance of graphite thin film materials *Measurement* **93** 1–17

[14] Tzeneva R 2012 Investigation of High Power Bolted Busbar Connectors with Longitudinal Slots *Przegląd Elektrotechniczny* 223–6

[15] Gao Z, Zhang X, Wang Y, Yang R, Wang G and Wang Z 2016 Measurement of the Poisson’s ratio of materials based on the bending mode of the cantilever plate *BioResources* **11** 5703–21

[16] Kraftmakher Y 2018 The inverse method of measuring resistivity in a rotating magnetic field: A student project *Eur. J. Phys.* **39**

[17] Alvarado S, Marín E, Juárez A G, Calderón A and Ivanov R 2012 A hot-wire method based thermal conductivity measurement apparatus for teaching purposes *Eur. J. Phys.* **33** 897–906

[18] Laor A, Herrell P J and Mayer M 2015 A Study on Measuring Contact Resistance of Ball Bonds on Thin Metallization *IEEE Trans. Components, Packag. Manuf. Technol.* **5** 704–8

[19] Bringuier E 2013 The electrical resistance of vacuum *Eur. J. Phys.* **34** 931

[20] Riba J-R, Martínez J, Moreno-Eguilaz M and Capelli F 2021

Characterizing the temperature dependence of the contact resistance in substation connectors *Sensors Actuators A Phys.* **327** 112732
[21] Di Troia G, Woo K and Zahlman G 2007 *Connector Theory and Application: A Guide to Connection Design and Specification* ed Burndy (Londonderry, NH, USA: Burndy)